Journal of Nanoscience and Nanotechnology
Vol. 11, 6747–6756, 2011

Salts Responsive Nanovesicles Through π-Stacking Induced Self-Assembly of Backbone Modified Tripeptides

Pradyot Koley[1], Michael G. B. Drew[2], and Animesh Pramanik[1,*]

[1] *Department of Chemistry, University of Calcutta, 92, A. P. C. Road, Kolkata 700009, India*
[2] *School of Chemistry, The University of Reading, Whiteknights, Reading RG6 6AD, UK*

A set of backbone modified peptides of general formula Boc-Xx-*m*-ABA-Yy-OMe where *m*-ABA is *meta*-aminobenzoic acid and Xx and Yy are natural amino acids such as Phe, Gly, Pro, Leu, Ile, Tyr and Trp etc., are found to self-assemble into soft nanovesicular structures in methanol-water solution (9:1 by v/v). At higher concentration the peptides generate larger vesicles which are formed through fusion of smaller vesicles. The formation of vesicles has been facilitated through the participation of various noncovalent interactions such as aromatic π-stacking, hydrogen bonding and hydrophobic interactions. Model study indicates that the π-stacking induced self-assembly, mediated by *m*-ABA is essential for well structured vesicles formation. The presence of conformationally rigid *m*-ABA in the backbone of the peptides also helps to form vesicular structures by restricting the conformational entropy. The vesicular structures get disrupted in presence of various salts such as KCl, $CaCl_2$, N(n-Bu)$_4$Br and $(NH_4)_2SO_4$ in methanol-water solution. Fluorescence microscopy and UV studies reveal that the soft nanovesicles encapsulate organic dye molecules such as Rhodamine B and Acridine Orange which could be released through salts induced disruption of vesicles.

Keywords: Nanovesicles, Peptides, Self-Assembly, Responsive.

RESEARCH ARTICLE

1. INTRODUCTION

Design and construction of soft molecular assemblies that can respond to external stimulus are becoming increasingly important because of their diverse applications in drug delivery, carrying biologically relevant molecules and sensing various biochemical processes.[1–3] External stimuli such as temperature, pH, light, electric field, chemical and ionic strength may trigger disruption of soft assemblies by modifying shape and surface properties.[4–12] It has been observed that peptides are efficient building blocks for fabricating nanoscopic soft assemblies responsive to various external stimuli.[4–17] Generally amphiphilic small peptides self-assemble into nanovesicles in aqueous medium through interactions occurring between hydrophobic and hydrophilic parts.[18–21] Surfactant-like peptides also undergo self-assembly to form nanovesicles in polar solvent due to hydrophobic and hydrophilic interactions.[22–25] However, recent studies have demonstrated that the formation of nanostructures could also be facilitated through the participation of other non-covalent interactions such as hydrogen bonding and aromatic π-stacking, with or without the presence of hydrophobic effect.[26–33] Since these noncovalent interactions are complementary and effective in organic solvents, it opens a way to fabricate nanostructures in a more wider range of solvent systems. Several bioinspired designs of soft assemblies based on aromatic π–π interactions have been reported in recent times.[34–39] In this paper we are interested in developing simple molecular systems which will produce responsive supramolecular assemblies through hydrogen bonding and aromatic π-stacking induced self-assembly.

Keeping this in view several backbone modified tripeptides of general formula Boc-Xx-*m*-ABA-Leu-OMe (*m*-ABA: *meta*-aminobenzoic acid) where Xx is Phe in peptide **I**, Gly in peptide **II**, Pro in peptide **III**, Ile in peptide **IV** and Tyr in peptide **V** have been designed by incorporating *m*-aminobenzoic acid at the centre to invoke aromatic π–π interactions in the self-assembly (Fig. 1). At the same time the conformationally rigid *m*-ABA in the backbones of the peptides will help to produce supramolecular assemblies by restricting the conformational entropy.[18,40–45] Moreover the presence of *m*-ABA may provide proteolytic stability to the self-assembled supramolecular structures.[18] Peptides containing Leu at position 1 such as Boc-Leu-*m*-ABA-Yy-OMe, where Yy is Ile in peptide **VI** and Trp in peptide **VII** have also been designed to examine whether the self-assembly of all these

*Author to whom correspondence should be addressed.

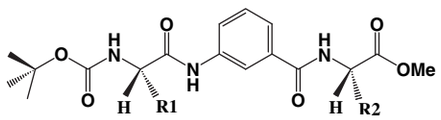

Peptide **I**: R1= -CH_2-C_6H_5, R2= -CH_2-CH-$(CH_3)_2$
Peptide **II**: R1= -H, R2= -CH_2-CH-$(CH_3)_2$
Peptide **IV**: R1= -CH(CH_3)-CH_2-CH_3, R2= -CH_2-CH-$(CH_3)_2$
Peptide **V**: R1= -CH_2-(C_4H_4)-*p*-OH, R2= -CH_2-CH-$(CH_3)_2$
Peptide **VI**: R1= -CH_2-CH-$(CH_3)_2$, R2= -CH(CH_3)-CH_2-CH_3
Peptide **VII**: R1= -CH_2-CH-$(CH_3)_2$ R2 = -CH_2-(3-indonyl)

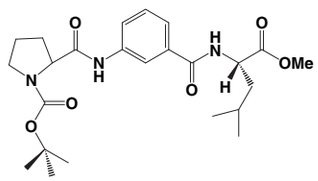

Peptide **III**

Fig. 1. Schematic representation of peptides **I–VII**.

peptides **I–VII** is sequence specific or not (Fig. 1). Model study has been carried out with peptides Boc-Leu-Phe-Ile-OMe (**VIII**) and Boc-Leu-Ile-Val-OMe (**IX**), where the centrally placed *m*-ABA has been replaced by natural amino acids to assess the role of *m*-ABA in the formation of supramolecular assemblies. The dye entrapment property and responsive behavior of the supramolecular assemblies to external stimuli have been explored.

RESEARCH ARTICLE

2. EXPERIMENTAL DETAILS

2.1. General Methods and Materials

All amino acids, *meta*-amino benzoic acid, HOBt (1-hydroxybenzotriazole) and DCC (dicyclohexylcarbodiimide) were purchased from Sigma chemicals.

2.2. Synthesis of the Peptides

The peptides were synthesized by conventional solution phase methodology.[46] The *t*-butyloxycarbonyl (Boc) group was used for N-terminal protection and the C-terminus was protected as the methyl ester. Couplings were mediated by N,N′-dicyclohexylcarbodiimide (DCC)/1-hydroxybenzotriazol (HOBT). Deprotection of the methyl ester was performed using the saponification method. All intermediates were characterized by thin layer chromatography on silica gel and used without further purification. Final peptides were purified by column chromatography using silica gel (100–200 mesh) as the stationary phase. Ethyl acetate and petroleum ether mixture was used as the eluent. The reported peptides **I–IX** were characterized by ^{1}H NMR spectroscopy, ^{13}C NMR spectroscopy, microanalysis and IR spectroscopy while the structures of peptides **I–III** were confirmed by X-ray crystallography.

(a) Boc-Phe-*m*-ABA-OMe (**1**). Initially N-terminal protection with Boc group of L-Phenyl alanine was performed using the literature method.[47] The fragment Boc-Phe-OH (1.5g, 5.66 mmol) was dissolved in a mixture of dichloromethane (DCM, 6 ml) and dimethylformamide (DMF, 5 ml). H-*m*ABA-OMe obtained from its hydrochloride (2.12 g, 11.31 mmol) was then added followed by addition of DCC (1.75 g, 8.49 mmol) and HOBT (0.76 g, 5.66 mmol) in ice-cold conditions. The reaction mixture was stirred at room temperature for 1 day. The precipitated N,N′-dicyclohexylurea (DCU) was filtered off. The organic layer was diluted with 30 ml ethyl acetate and washed with 1N HCl (3×30 ml), brine, 1M Na_2CO_3 solution (3×30 ml) and then again with brine. The solvent was dried over anhydrous Na_2SO_4 and evaporated *in vacuo* to give a waxy colorless solid. Yield: (2.0 g, 88.89%).

(b) Boc-Phe-*m*-ABA-OH (**2**). **1** (2.0 g, 5.02 mmol) was dissolved in methanol (20 ml) and 2N NaOH (10 ml) was added. The reaction mixture was stirred for 1 day at room temperature. The progress of the reaction was monitored by TLC. After completion of reaction the methanol was evaporated. The residue was diluted with water and washed with diethyl ether. The aqueous layer was cooled in an ice-bath and then neutralized by using 2N HCl and extracted with ethyl acetate. The solvent was evaporated *in vacuo* to give a waxy colorless solid. Yield: (1.75 g, 90.67%).

(c) Boc-Phe-*m*-ABA-Leu-OMe (peptide **I**). **2** (1.75 g, 4.56 mmol) was dissolved in DMF (10 ml). Leu-OMe obtained from its hydrochloride (1.65 g, 9.09 mmol) was added, followed by addition of DCC (1.41 g, 6.84 mmol) and HOBT (0.62 g, 4.58 mmol) in ice-cold conditions. The reaction mixture was stirred at room temperature for 2 days. The precipitated DCU was filtered off. The organic layer was diluted with 30 ml ethyl acetate and washed with 1N HCl (3×30 ml), brine, 1M Na_2CO_3 solution (3×30 ml) and then again with brine. The solvent was then dried over anhydrous Na_2SO_4 and evaporated *in vacuo*, to give a colorless solid compound. Purification was done using silica gel as stationary phase and ethyl acetate-petroleum ether mixture as eluent. Single crystals were grown from $CHCl_3$-petroleum ether mixture by slow evaporation.

Yield: (2.1 g, 90.13%). Mp = 120–122 °C (from $CHCl_3$-petroleum ether); IR ν_{max}(KBr)/cm^{-1} : 3297, 3063, 2958, 1749, 1674, 1548, 1445; ^{1}H NMR (300 MHz, $CDCl_3$, 25 °C, TMS) δ ppm: 9.27 (1 H, s, *m*-ABA (2) NH); 7.92 (1 H, d, J = 7.8 Hz, *m*-ABA (2) Hd); 7.75 (1 H, s, *m*-ABA (2) Ha); 7.16–7.36 (7 H, m, *m*-ABA (2) Hb, Hc and Phe (1) phenyl ring protons); 6.83 (1 H, br, Leu (3) NH); 5.09 (1 H, d, J = 7.5 Hz, Phe (1) NH); 4.67–4.74 (2 H, m, Leu (3) & Phe (1) C^{α}Hs); 3.81 (3 H, s, –OCH_3); 3.04–3.21 (2 H, m, Phe (1) C^{β}Hs); 1.63–1.67 (2 H, m, Leu (3) C^{β}Hs); 1.38 (9 H, s, Boc CH_{3S}); 0.83-0.97 (7 H, m, Leu (3) C^{γ}H and C^{δ}Hs).

^{13}C NMR (75 MHz, $CDCl_3$)δ ppm: 173.87, 171.35, 167.55, 156.69, 136.98, 135.73, 134.73, 129.38, 129.20 (2C), 128.78 (2C), 127.25, 124.08, 123.05, 117.31, 81.07, 56.21, 52.15, 51.50, 40.49, 38.54, 28.30 (3C), 24.77, 23.29, 21.19.

Anal. Calcd for $C_{28}H_{37}N_3O_6$: C, 65.73; H, 7.29; N, 8.21. Found: C, 65.66; H, 7.22; N, 8.17%.

Synthesis and characterization of peptides **II–IX** were carried out using the same procedure.

2.3. Characterization Techniques

2.3.1. Scanning Electron Microscopy (SEM).

SEM and FE-SEM imaging were carried out to investigate the morphology of the nanostructures. In general, freshly prepared solutions of peptides (10.0 mM) in methanol-water (9:1 by v/v) were taken on glass cover slips and evaporated to dryness for 24 hours. A gold coating was applied to the top of the samples to make it conductive for analysis. Then, SEM measurements were performed on a S3400N, HITACHI, JAPAN instrument and JEOL JSM-6700F instrument at 5.0 kV to 10.0 kV voltage and 5000 × to 40 000 × magnification. For salts triggered disruption studies 10.0 mM solutions of various salts such as KCl, $CaCl_2$, $N(n\text{-}Bu)_4Br$ and $(NH_4)_2SO_4$ in methanol-water (1:1 by v/v) were added into the freshly prepared 10.0 mM methanol-water solution of peptide **I** in 1:1 (v/v) proportion and incubated for 12 hours and followed by scanning electron microscopic imaging.

2.3.2. High Resolution Transmission Electron Microscopy (HR-TEM)

High resolution transmission electron microscopy (HR-TEM) was also carried out to investigate the morphology of nanostructures. Freshly prepared solutions of peptides (6.0 mM) in methanol-water (9:1 by v/v) were sonicated with UC 250W, INECO ultrasonicator for 30 mins, and one drop of each of these solutions was taken in a carbon-coated copper grid (300 mesh) and evaporated to dryness under vacuum for 12 hours. With these grids TEM studies were carried out using a JEOL JEM-2100 electron microscope and TECNAI G2 SPIRIT Bio TWIN electron microscope with 80 kV operating voltage. For salts triggered disruption studies, 6.0 mM solutions of various salts such as KCl, $CaCl_2$, $N(n\text{-}Bu)_4Br$ and $(NH_4)_2SO_4$ in methanol-water (1:1 by v/v) were added into the freshly prepared 6.0 mM methanol-water solution of peptide **I** in 1:1 (v/v) proportion and incubated for 12 hours followed by transmission electron microscopic imaging.

2.3.3. Atomic Force Microscopy (AFM)

One drop (10 μL) of freshly prepared methanol-water (9:1 by v/v) solutions of peptides **I–III** (6.0 mM) was transferred onto a freshly cleaved mica surface and the sample coated mica was dried for 12 hours at room temperature. With these samples coated mica surfaces, AFM studies were carried out using a VEECO, Multimode, Nanoscope-IIIA atomic force microscope operating under Tapping mode (RTESP Tip). The force constant was 20–80 N m^{-1}, while the resonant frequency was 286.17 kHz.

2.3.4. Dynamic Light Scattering (DLS) Measurements

Freshly prepared solutions of peptides **I–III** (6.0 mM) in methanol-water (9:1 by v/v) were used for dynamic light scattering measurements using a Nano-S-1600, MALVERN, USA instrument, after ultrasonication of the solutions for 30 min.

2.3.5. Thermogravimetric Analysis (TGA)

A solution of peptide **I** (6.5 mg mL^{-1}) in methanol-water (9:1 by v/v) was aged for 7 days in open air at r. t. and then dried under vacuum. This sample was analyzed on a Mettler Toledo TGA/SDTA 851 thermal analyzer in a dynamic atmosphere of dinitrogen (flow rate = 30 cm^3 min^{-1}). The sample was heated in an alumina crucible at a rate of 5 °C min^{-1}.

2.3.6. Fluorescence Microscopy and UV Studies

A mixture of solution of peptide **I** in methanol-water (9:1 by v/v) and Rhodamine B in a 1:1 v/v ratio (final concentration of each of the substance being 10^{-4} M) was incubated for 1 day at r. t. After 1 day one drop (20 μL) of the solution was loaded on the glass slide and dried at r. t. under vacuum. The excess dye was removed from glass slide by repeated washing with deionized water. Then the dye loaded glass slide was dried at r. t. under vacuum. Finally these dye entrapped vesicular structures were examined under a fluorescence microscope (Fluorescence Microscope Olympus BX 61). Similar experiment was done with the dye Acridine Orange also. For salt triggered disruption studies, solutions of various salts in methanol-water (9:1 by v/v) were added on the 1 day aged solution of peptide **I** and Rhodamine B (final concentration of each of the substance being $\sim 10^{-4}$ M) and the resultant solution was incubated for 12 hours. After that one drop (20 μL) of the solution was loaded on the glass slide and dried at r. t. under vacuum. Finally the ruptured vesicles and release of dyes were examined on the same fluorescence microscope.

The Fluorescence emission spectra (730–530 nm) of peptide **I** was recorded in methanol-water solution (9:1 by v/v) with a Fluorescence Spectrometer Perkin Elmer LS 55 using ~1% Attenuator Assy. The spectrums were taken using an excitation wavelength of 540 nm. The electronic absorption spectra (800–200 nm) of the peptides were recorded in methanol-water solution (9:1 by v/v) with a Hitachi U-3501 spectrophotometer.

2.3.7. Single Crystal X-ray Diffraction Study

Diffraction data for the three peptides **I**, **II** and **III**, were obtained with MoKα radiation at 150 K using the Oxford Diffraction X-Calibur CCD System. The crystals were positioned at 50 mm from the CCD. 321 frames were measured with a counting time of 10 s. Data analyses were carried out with the Crysalis program.[48] The structures were solved using direct methods with the Shelxs97 program.[49] Non-hydrogen atoms were refined with anisotropic thermal parameters. The hydrogen atoms bonded to carbon were included in geometric positions and given thermal parameters equivalent to 1.2, or 1.5 times for methyl groups, times those of the atom to which they were attached. There was disorder in parts of the side groups in peptide **I** which also contained two water molecules, refined with 50% occupancy. The structures were refined on F^2 using Shelxl97.[49] The CIF files of the 3 structures have been deposited at the Cambridge Crystallographic Data Centre with reference numbers CCDC 767778 to 767780 inclusive.

3. RESULTS AND DISCUSSION

3.1. Single Crystal X-ray Diffraction and UV Studies of Self-Assembly

The single crystal X-ray diffraction studies of the crystals of peptides **I–III** grown from $CHCl_3$-petroleum ether mixture revealed that all three structures, though not isomorphous, contained four molecules, named **A**, **B**, **C**, **D** in the asymmetric unit. All the molecules adopt similar extended structures with the centrally placed *m*-ABA providing an all *trans* extended configuration. In the solid state all three structures form dimers *via* π–π interactions between the phenyl rings of *m*-ABA. In peptide **I**, the two phenyl rings intersect at angles of 15.7° in the **AB** dimer and 16.4° in the **CD** dimer with closest C…C contacts of 3.55, 3.48 Å respectively. In peptide **II**, angles are 30.8° and 15.8° and shortest distances 3.56, 3.50 Å respectively (Fig. 2(a)) while in peptide **III**, dimensions are 15.7°, 16.4°, 3.55, 3.48 Å respectively. The dimers are further stabilized by four strong intermolecular hydrogen bonds between Boc-CO…H-N-*m*-ABA and Xx(1)-CO…H-N-Leu (Fig. 2(a)). The formation of these molecular dimers **AB** and **CD**, described above, is common to all three peptides but further packing of the dimers facilitated by hydrogen bond formation involving N(3) is dependent upon the nature of the further residues in the peptides.

The dimers of peptides **I–III** are packed into β-sheet layers through intermolecular hydrogen bonds and van der Waals interactions (Fig. 2(b)). The solid state packing clearly demonstrates that all the peptides **I–III** form layers of β-sheets through molecular self-assembly stabilized by various noncovalent interactions such as aromatic π–π interactions, hydrogen bonding and van der Waals interactions. It has been proposed that the closure of the

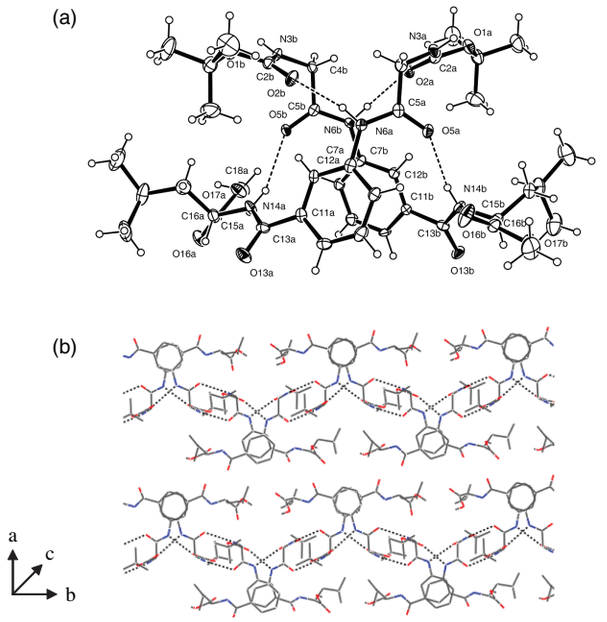

Fig. 2. (a) The molecular duplex of peptide **II** in the solid state formed through aromatic π–π interactions and hydrogen bonds, shown as dotted lines; (b) Packing pattern of peptide **II** showing the formation β-sheet layer in the *ab* plane.

β-sheet layers along two axes may lead to the formation of spherical structures under suitable condition.[20]

The existence of aromatic π-stacking interactions in the solid state was further probed by UV studies. The highly diluted methanolic solutions (0.015 mM) of the peptides **I–III** show absorption maxima around 225 nm due to aromatic chromophore (Fig. 3), where the peptide molecules are not self-assembled and there are no π-stacking interactions. But the solid materials of peptides **I–III** grown from methanol-water show absorption maxima around 305 nm. The substantial red shift (~80 nm) on going from solution to solid state may be attributed to

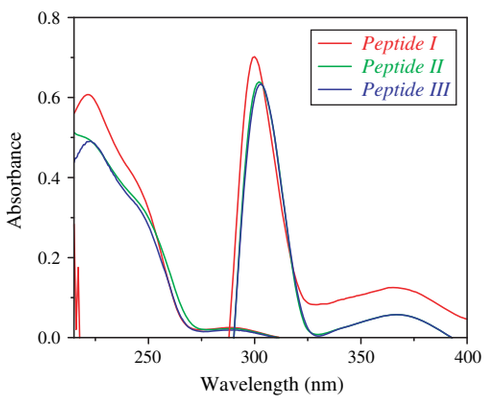

Fig. 3. UV absorption spectra indicate a significant red shift (~ 80 nm) on going from solution (0.015 mM) to vesicular solid state of peptide **I–III** due to aromatic π–π interactions.

the π-stacking interactions among the aromatic rings in the solid state due to self-assembly.[50]

3.2. SEM, TEM and AFM Studies

The scanning electron micrographs (SEM) reveal that the peptides **I–III** can generate spherical objects from $CHCl_3$-petroleum ether mixture (3:7 by v/v), but the spheres are found in aggregated form (data not shown). Therefore we decided to use more polar methanol-water mixture (9:1 by v/v) for generating isolated spherical objects. The SEM images show that the peptides **I–V** generate well structured spherical objects of an average diameter 0.5–2 μm, when freshly prepared methanol-water (9:1 by v/v) solutions of peptides (10.0 mM) were dried on glass surfaces by slow evaporation (Figs. 4(a–c), representative data shown). Peptides **VI** and **VII** where Leu has been placed at position 1 and Ile and Trp at position 3 also show similar sphere forming properties (data not shown), indicating that there is no restriction in choosing the first and third residues of the peptides for these spherical structures formations as long as they are hydrophobic in nature. Interestingly the SEM images of the peptides also reveal some cracked and opened-up hollow spheres which indicate the hollow nature of the spherical objects (Figs. 4(b and d)). These porous structures are formed when the trapped volatile solvent such as methanol escapes from the surface during the drying process.[51–56] This phenomenon is quite similar to that observed when engendering porosity in polymer samples with the help of porogens.[57]

The SEM studies confirm that the peptides **VIII** and **IX** where the centrally placed *m*-ABA has been replaced by natural hydrophobic amino acids can not produce well-structured spherical objects from methanol-water (9:1 by v/v) solutions. The result indicates that the π-stacking induced self-assembly, mediated by *m*-ABA is essential for well structured spherical objects formation. The conformational constrain induced by *m*-ABA plays an important role in the formation of supramolecular spherical assemblies by restricting the conformational entropy. Although hydrophobic interaction helps in the self-assembly, this alone cannot lead to the formation of well-structured spherical objects as evident from the results of peptides **VIII** and **IX**.

The TEM studies reveal that the peptides **I–III** form vesicular structures from 6.0 mM solutions of peptides in methanol-water (9:1 by v/v) with an average diameter 20–200 nm (Figs. 5(a and b), representative data shown), which is much less than the average diameter observed in SEM studies (Fig. 4). TEM images clearly indicate the layer-like boundary and hollow nature of self-assembled structures of the peptides (Fig. 5). Therefore the spherical objects observed in the SEM images are actually vesicles. The results indicate that the size of the vesicles is dependent on concentration of the peptides. At higher concentration (10.0 mM) larger vesicles are formed through the fusion of smaller vesicles, which is evident from the SEM images where fused vesicles are observed (data not shown). The time-dependent SEM imaging of peptide **II** after 6 hrs and 24 hrs clearly shows the intermediate structures affording vesicle fusion (Fig. 6). TEM images of peptides **I** and **II** at higher concentration (10.0 mM) also show the formation of larger vesicles (~400–800 nm) (Fig. 5(c), representative data shown). Interestingly, some intermediate states of fused vesicles of peptide **II** are also observed in the TEM image (Fig. 5(d)). The AFM studies of peptides **I–III** with 6.0 mM solutions in methanol-water (9:1 by v/v) show the formation of vesicular structures with an average diameter 20–200 nm (Fig. 7(a), representative data shown).

3.3. Dynamic Light Scattering (DLS) Studies

To probe the size distributions of nanovesicles in the solution phase, DLS experiments were carried out with 6.0 mM solutions of peptides **I–III** in methanol-water (9:1 by v/v), after ultrasonication of the solutions for 30 min. Although SEM and TEM studies reveal the formation of both bigger and smaller nanovesicles simultaneously, DLS data demonstrate the formation of monodispersed vesicles with a distribution of hydrodynamic diameters centered on 85.0 nm in peptide **I**, 105.7 nm in peptide **II** and 164.2 nm in peptide **III** (Fig. 7(b), representative data shown). Significantly all the peptides **I–III** generate small sized nanovesicles in the solution phase compared to vesicles generated on the solid surfaces.

To examine the fusion process of the vesicles in the solution phase time-dependent DLS measurements were carried out with a 10.0 mM solution of peptide **II** in methanol-water (9:1 by v/v). The distributions of hydrodynamic diameters with the increase in time are plotted in Figure 8(a). The plot clearly shows that the hydrodynamic diameter of the vesicles increases steadily upto 24 hrs after that the fusion of vesicles stops as there is no further significant change in diameter. The plot of hydrodynamic diameters of vesicles against time shows a consistent increase in the size of the vesicles upto 24 hrs (Fig. 8(b)).

3.4. Thermo Gravimetric (TGA) and Differential Thermal Analysis (DTA)

The TGA thermogram of representative peptide **I** nanovesicles shows ~21% weight loss between room temperature and ~240 °C (Fig. 9). This may be attributed to the loss of methanol and water from the confines of peptide vesicular structures. The result indicates that the vesicular structures are stable up to 240 °C, after which the peptide decomposes. The DTA plot shows that the loss of solvent molecules from the vesicular structures is an endothermic process.

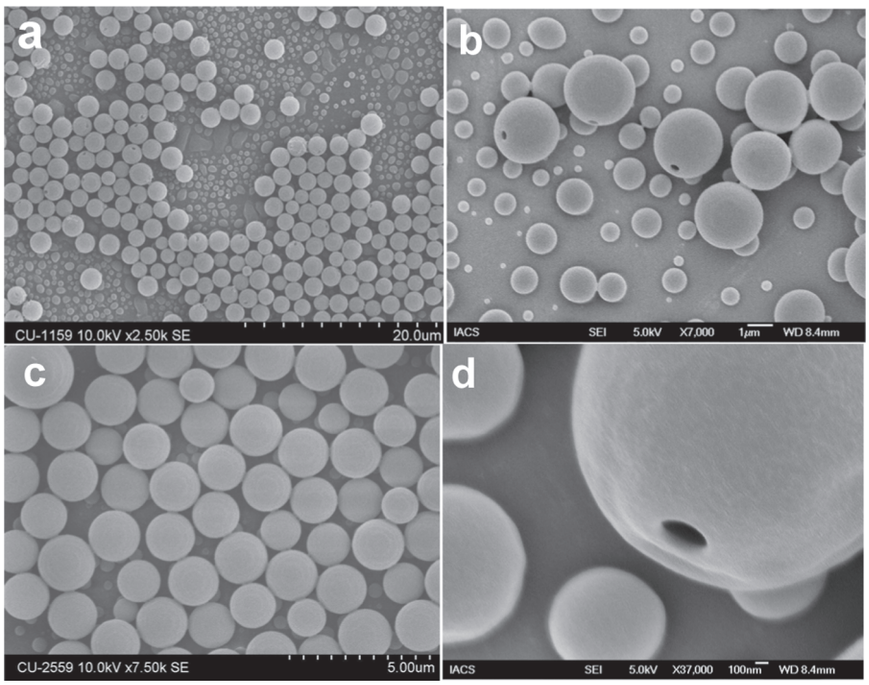

Fig. 4. SEM images of nanovesicles of (a) peptide **I**, (b) peptide **IV** and (c) peptide **V**, generated from methanol-water (9:1 by v/v) solution (10.0 mM); (d) Showing the hollow sphere of peptide **IV**.

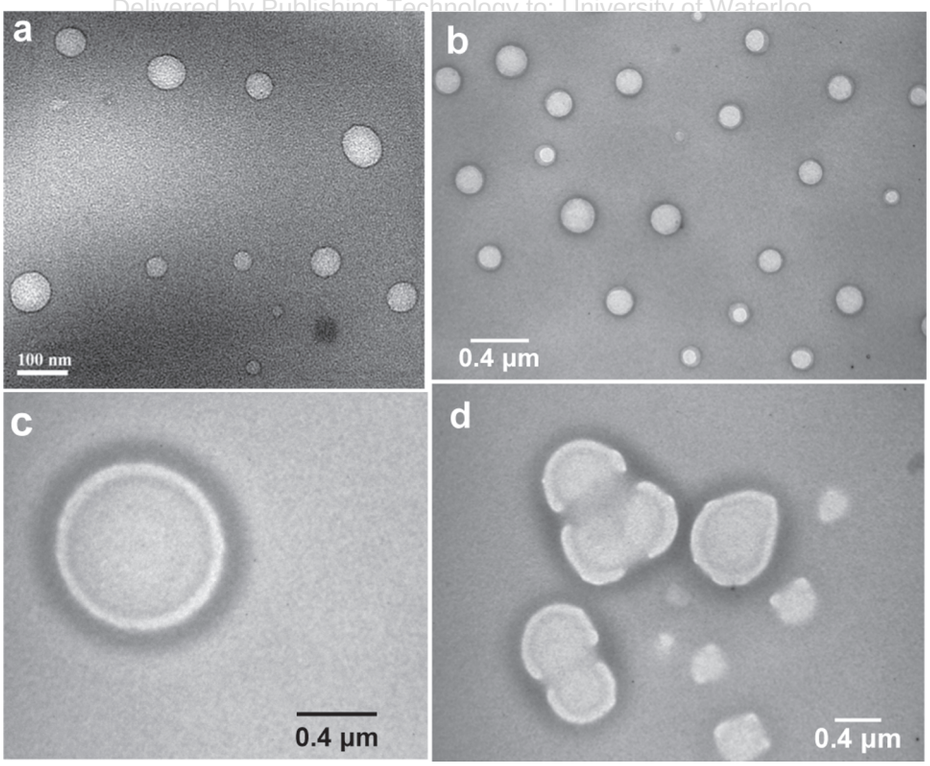

Fig. 5. HR-TEM images of nanovesicles of (a) peptide **I** and (b) peptide **II** generated from 6.0 mM methanol-water (9:1 by v/v) solutions of peptides; (c) TEM image of bigger nanovesicles of peptide **II** at higher magnification generated from 10.0 mM solution; (d) TEM image of fused vesicles of peptide **II**.

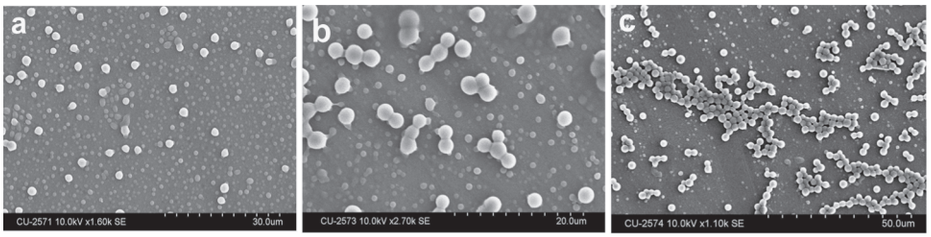

Fig. 6. Time-dependent SEM images of peptide **II** (a) freshly prepare solution, (b) after 6 hrs and (c) after 24 hrs, showing the intermediate structures affording fusion.

3.5. Formation and Disruption of Vesicles

It is evident from the TEM, SEM, and AFM images that the hydrophobic peptides **I–VII** with centrally placed *m*-ABA generate vesicular structures from polar methanol-water mixture. The *m*-ABA mediated π-stacking interactions play an important role in the self-assembly. Interestingly, the role of aromatic π-stacking interactions in providing energetic contributions as well as directionality has been proposed for self-assembled protein/peptide aggregates.[58] Crystal packing shows that the peptides **I–III** form β-sheet layers through molecular self-assembly (Fig. 2(b), representative data shown). The formation of nanovesicles may be envisaged by considering the closure of the β-sheet-like layers in two different directions simultaneously as illustrated in Figure 10.[20, 21] At higher concentration (10.0 mM), the peptides form bigger vesicles which are formed through the fusion of small vesicles. The driving forces behind the fusion process may be the release of strain in the initially formed vesicles, which have high curvature. By fusion into larger vesicles, curvature energy decreases, thus leading to a thermodynamically more stable state.[59]

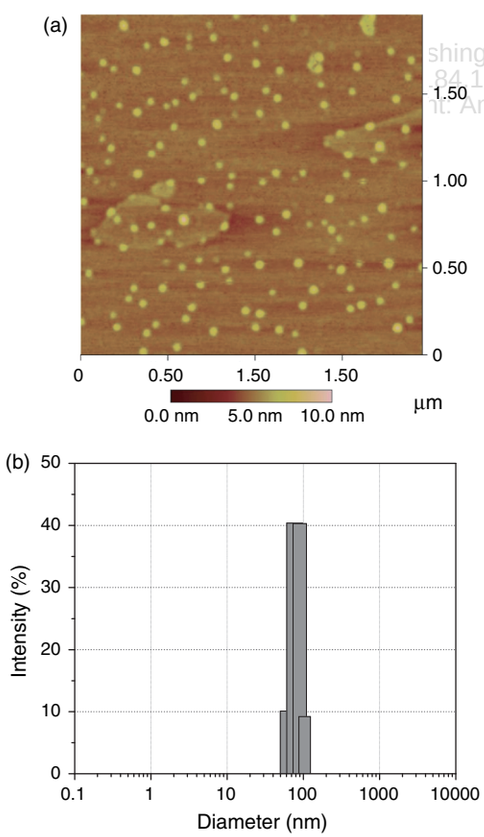

Fig. 7. (a) AFM topography image and (b) distribution diameter of nanovesicles of peptides **I** in DLS study of 6.0 mM methanol-water (9:1 by v/v) solution of peptide.

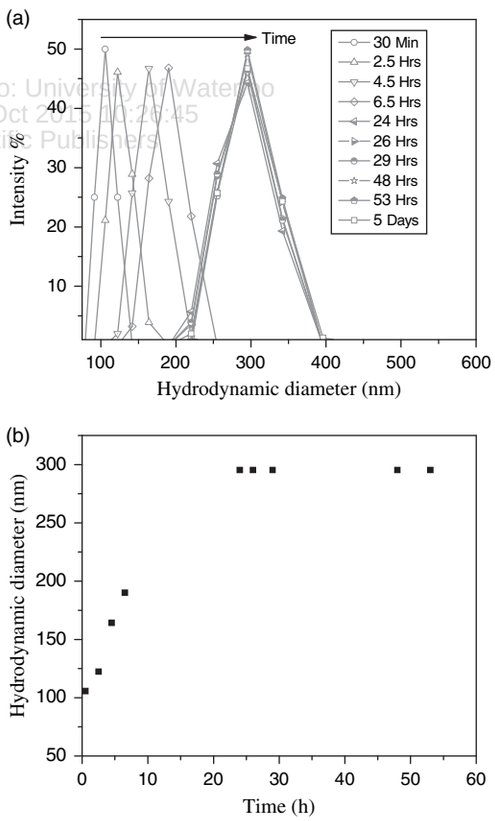

Fig. 8. (a) Plot showing the distributions of hydrodynamic diameters of the nanovesicles of peptide **II** in 10.0 mM methanol-water (9:1 by v/v) solution at different time in DLS study; (b) Plot showing the variation of hydrodynamic diameter of the vesicles of peptide **II** with time. Hydrodynamic diameters of highest intensities were plotted against time.

RESEARCH ARTICLE

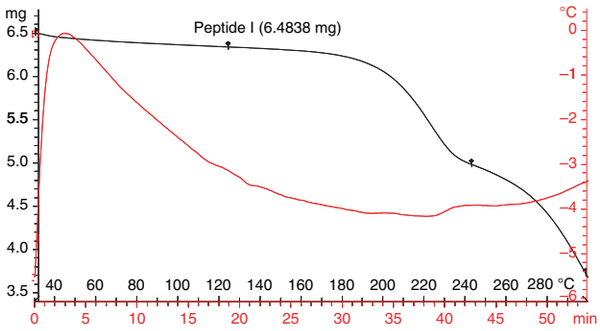

Fig. 9. The black curve indicates TGA and red curve indicates DTA.

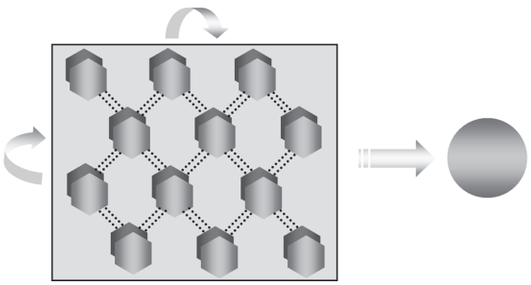

Fig. 10. Schematic representation of a possible mode of vesicle formation from β-sheet layers of peptides.

In order to understand the driving forces for such self-assembly and the softness of the vesicular structures, the salts triggered disruption studies were carried out.[34, 60] In this experiment methanol-water solutions of various salts such as KCl, $CaCl_2$, $N(n\text{-}Bu)_4Br$ and $(NH_4)_2SO_4$ (6–10 mM) were added into freshly prepared methanol-water solutions of peptide **I** (6–10 mM) separately and incubated for 12 hours and followed by SEM and TEM imaging. In all cases disruption of nanovesicles were observed (Figs. 11(a and b)). The addition of salts to the solutions causes the simultaneous breakage of various weak noncovalent interactions present in the vesicular structures, such as aromatic π-stacking, hydrogen bonding and hydrophobic interactions.[61] All these effects together lead to the disruption of nanovesicles.

3.6. Encapsulation and Release of Dyes

Entrapment of organic dye molecules such as Rhodamine B and Acridine Orange within the vesicular structures of peptide **I** has been examined.[21, 34, 35, 62, 63] A methanol-water (9:1 by v/v) solution of Rhodamine B was added to a methanol-water (9:1 by v/v) solution of peptide **I** so that the final concentration of each substance was maintained at $\sim 10^{-4}$ M in the resultant solution. One drop of the one day aged above solution was loaded on a glass slide and dried at room temperature and then examined under fluorescence microscope after washing out the excess dyes with deionized water for several times. Similar study was carried out with Acridine Orange also. Visualization of the Rhodamine B and Acridine Orange entrapped vesicular structures strongly supports the encapsulation phenomenon (Figs. 11(c and e)). This phenomenon was further confirmed by fluorescence emission study. Initially the fluorescence emission spectra of a 10^{-4} M solution of pure Rhodamine B in methanol-water (9:1 by v/v) solution was recorded, which showed emission band around 570 nm (Fig. 12(a)). Then fluorescence emission spectra of a methanol-water (9:1 by v/v) solution of Rhodamine B and peptide **I**, where the concentration of

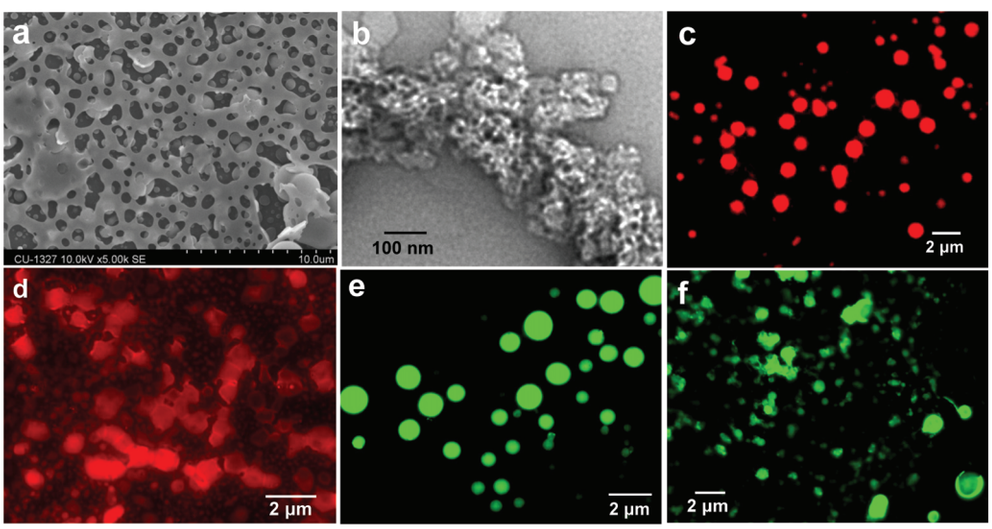

Fig. 11. (a) SEM and (b) TEM images of ruptured vesicles of peptide **I** after addition of KCl solution and incubation for 12 hours; and (c) Rhodamine B entrapped nanovesicles of peptide **I** observed under fluorescence microscope (one day aged solution of dye-loaded vesicles); (d) fluorescence microscopic image of ruptured vesicle after addition of KCl solution to the dye loaded vesicular solution of peptide **I** and incubation for 12 hours. (e) and (f) are the fluorescence images of Acridine Orange dye loaded and ruptured nanovesicles of peptide **I** respectively.

RESEARCH ARTICLE

each substance was maintained at $\sim 10^{-4}$ M was recorded. In first 3 hours no significant change was observed in the fluorescence intensity compared to the pure Rhodamine B solution. After 4 hours the fluorescence intensity decreased steadily over next 8 hours showing encapsulation of dye molecules by the vesicles (Fig. 12(a)). Further the dye loaded vesicular structures of peptide **I** were found to get disrupted in presence of KCl causing the release of entrapped Rhodamine B when observed under fluorescence microscope (Fig. 11(d)). Similarly the rapture of Acridine Orange loaded vesicles of peptide **I** by KCl was also observed by fluorescence microscopy (Fig. 11(f)). The encapsulation of Acridine Orange by the vesicles of peptides **I** was confirmed by recording UV absorption spectra, in which a steady decrease of absorption intensity of Acridine Orange with time was observed upto 12 hours (Fig. 12(b)). The initial enhancement in the absorbance after addition of dye may be due to weak interactions between dye and peptide molecules.

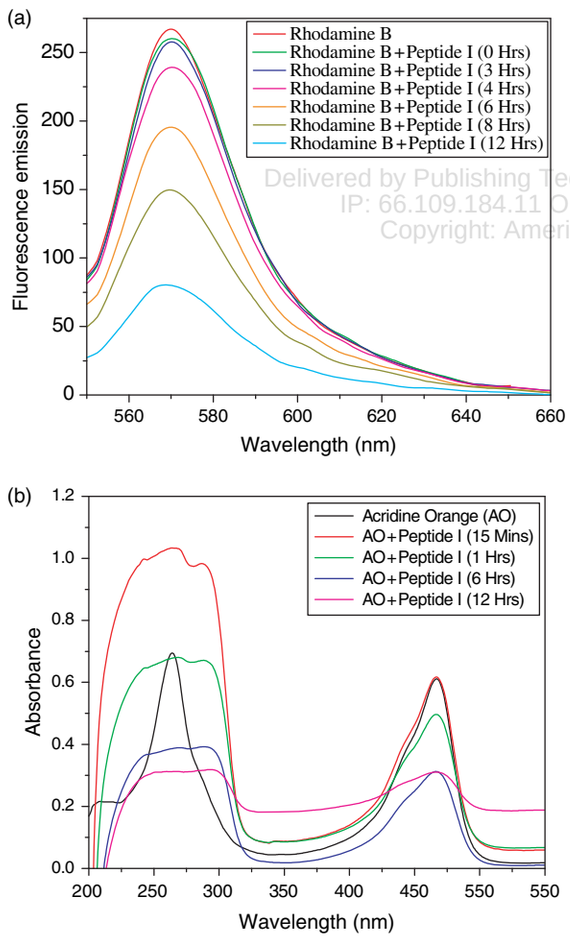

Fig. 12. (a) Fluorescence emission spectra showing the encapsulation of Rhodamine B dye by the vesicles of peptide **I** in methanol-water and (b) UV absorption spectra showing the encapsulation of Acridine Orange dye by peptide **I**.

4. CONCLUSION

It has been observed that the backbone modified peptides of general formula Boc-Xx-*m*-ABA-Yy-OMe (*m*-ABA: *meta*-aminobenzoic acid) where Xx and Yy are natural amino acids such as Phe, Gly, Pro, Leu, Ile, Tyr and Trp etc. can self-assemble into soft nanovesicular structures in methanol-water solution. The formation of vesicles has been facilitated through the participation of various noncovalent interactions such as aromatic π-stacking, hydrogen bonding and hydrophobic interactions. The model study indicates that the π-stacking induced self-assembly, mediated by *m*-ABA is essential for well structured vesicles formation. The conformational constrain induced by *m*-ABA plays an important role in the formation of nanovesicles by restricting the conformational entropy. Although hydrophobic interaction helps in the self-assembly, this alone cannot lead to the formation of well-structured vesicles as evident from the results of peptides **VIII** and **IX**, where *m*-ABA is replaced by natural amino acids. The vesicular structures are responsive to various salts such as KCl, $CaCl_2$, $N(n\text{-}Bu)_4Br$ and $(NH_4)_2SO_4$and can be disrupted by the simple addition of them. Fluorescence microscopy and UV studies reveal that the nanovesicles can encapsulate dye molecules which could be released by addition of salts. These soft nanovesicles may find applications as delivery vehicles for entrapment and transport of natural and unnatural molecules. Currently extensive research interest has been directed towards studies of vesicle fusion.[64, 65] It has been observed that larger vesicles are formed through fusion of small vesicles. This may be utilized for the model study to gain more insights about the formation, transport, and targeted fusion of endosomal vesicles in cell-free conditions.

Acknowledgments: The financial assistance of UGC, New Delhi is acknowledged [Major Research Project, No. 32-190/2006(SR)]. We acknowledge the financial assistance of *Centre for Research in Nanoscience & Nanotechnology (CRNN)*, University of Calcutta. We thank Dr. Prabir K. Maiti and Anirban Chakraborty of C. U. for providing SEM (TEQIP) and AFM (TEQIP) instrumental facilities. Pradyot Koley would like to thank CRNN for a senior research fellowship (SRF). We thank EPSRC and the University of Reading, UK for funds for Oxford Diffraction X-Calibur CCD diffractometer.

References and Notes

1. C. de las, H. Alarcón, S. Pennadam, and C. Alexander, *Chem. Soc. Rev.* 34, 276 **(2005)**.
2. R. Yerushalmi, A. Scherz, M. E. van der Boom, and H.-B. Kraatz, *J. Mater. Chem.* 15, 4480 **(2005)**.
3. N. Nath and A. Chilkoti, *Adv. Mater.* 14, 1243 **(2002)**.
4. B. Ozbas, J. Kretsinger, K. Rajagopal, J. P. Schneider, and D. J. Pochan, *Macromolecules* 37, 7331 **(2004)**.
5. C. J. Bosques and B. Imperiali, *J. Am. Chem. Soc.* 125, 7530 **(2003)**.

RESEARCH ARTICLE

6. S. Murdan, *J. Controlled Release* 92, 1 (**2003**).
7. J. H. Collier, B.-H. Hu, J. W. Ruberti, J. Zhang, P. Shum, D. H. Thompson, and P. B. Messersmith, *J. Am. Chem. Soc.* 123, 9463 (**2001**).
8. A. F. Dexter, A. S. Malcolm, and A. P. J. Middelberg, *Nat. Mater.* 5, 502 (**2006**).
9. J. R. Lu, S. Perumal, I. Hopkinson, J. R. P. Webster, J. Penfold, W. Hwang, and S. Zhang, *J. Am. Chem. Soc.* 126, 8940 (**2004**).
10. Y. Tachibana, M. Kurisawa, H. Uyama, and S. Kobayashi, *Biomacromolecules* 4, 1132 (**2003**).
11. W. Frey, D. E. Meyer, and A. Chilkoti, *Adv. Mater.* 15, 248 (**2003**).
12. F. Checot, S. Lecommandoux, Y. Gnanou, and H.-A. Klok, *Angew. Chem. Int. Ed.* 41, 1339 (**2002**).
13. A. K. Barman and S. Verma, *Chem. Commun.* 46, 6992 (**2010**).
14. E. G. Bellomo, M. D. Wyrsta, L. Pakstis, D. J. Pochan, and T. J. Deming, *Nat. Mater.* 3, 244 (**2004**).
15. R. Fairman and K. S. Aakerfeldt, *Curr. Opin. Struct. Biol.* 15, 453 (**2005**).
16. X. Zhao and S. Zhang, *Trends Biotechnol.* 22, 470 (**2004**).
17. K. Rajagopal and J. P. Schneider, *Curr. Opin. Struct. Biol.* 14, 480 (**2004**).
18. A. Mishra, J. J. Panda, A. Basu, and V. S. Chauhan, *Langmuir* 24, 4571 (**2008**).
19. J. Naskar and A. Banerjee, *Chem. Asian J.* 4, 1817 (**2009**).
20. M. Reches and E. Gazit, *Nano Lett.* 4, 581 (**2004**).
21. P. P. Bose, A. K. Das, R. P. Hegde, N. Shamala, and A. Banerjee, *Chem. Mater.* 19, 6150 (**2007**).
22. S. Santoso, W. Hwang, H. Hartman, and S. Zhang, *Nano Lett.* 2, 687 (**2002**).
23. R. Jayakumar, M. Murugesan, and M. R. Ahmed, *Bioorg. Med. Chem. Lett.* 10, 1547 (**2000**).
24. S. Vauthey, S. Santoso, H. Gong, N. Watson, and S. Zhang, *Proc. Natl. Acad. Sci. USA* 99, 5355 (**2002**).
25. J. N. Israelachvili, D. J. Mitchell, and B. W. Ninham, *Biochim Biophys Acta.* 470, 185 (**1977**).
26. W. Cai, G.-T. Wang, Y.-X. Xu, X.-K. Jiang, and Z.-T. Li, *J. Am. Chem. Soc.* 130, 6936 (**2008**).
27. L.-Y. You, X.-K. Jiang, and Z.-T. Li, *Tetrahedron* 65, 9494 (**2009**).
28. C. Wang, S. Yin, S. Chen, H. Xu, Z. Wang, and X. Zhang, *Angew. Chem. Int. Ed.* 47, 9049 (**2008**).
29. A. Ajayaghosh, P. Chithra, and R. Varghese, *Angew. Chem. Int. Ed.* 46, 230 (**2007**).
30. X. Yan, Y. Cui, Q. He, K. Wang, J. Li, W. Mu, B. Wang, and Z.-C. Ou-Yang, *Chem. Eur. J.* 14, 5974 (**2008**).
31. B.-S. Kim, D.-J. Hong, J. Bae, and M. Lee, *J. Am. Chem. Soc.* 127, 16333 (**2005**).
32. S. Mukhopadhyay, U. Maitra, I. G. Krishnamoorthy, J. Schmidt, and Y. Talmon, *J. Am. Chem. Soc.* 126, 15905 (**2004**).
33. A. Ajayaghosh, S. J. George, and V. K. Parveen, *Angew. Chem. Int. Ed.* 42, 332 (**2003**).
34. S. Ghosh, S. K. Singh, and S. Verma, *Chem. Commun.* 22, 2296 (**2007**).
35. S. Ghosh, P. Singh, and S. Verma, *Tetrahedron* 64, 1250 (**2008**).
36. K. B. Joshi and S. Verma, *Angew. Chem. Int. Ed.* 47, 2860 (**2008**).
37. S. Aravinda, N. Shamala, R. Rajkishore, H. N. Gopi, and P. Balaram, *Angew. Chem. Int. Ed.* 41, 3863 (**2002**).
38. C. A. Hunter, K. R. Lawson, J. Perkins, and C. J. Urch, *J. Chem. Soc., Perkin Trans.* 2, 651 (**2001**).
39. J. P. Gallivan and D. A. Dougherty, *Proc. Natl. Acad. Sci. USA* 96, 9459 (**1999**).
40. M. Antonietti and S. Förster, *Adv. Mater.* 15, 1323 (**2003**).
41. S. Foster and M. Schmidt, *Adv. Polym. Sci.* 120, 51 (**1995**).
42. S. Forster, V. Abetz, and H. E. Muller, Advance in Polymer Science, Springer, Berlin (**2004**), p. 173.
43. S. A. Jenekhe and X. L. Chen, *Science* 283, 372 (**1999**).
44. S. A. Jenekhe and X. L. Chen, *Science* 279, 1903 (**1998**).
45. S. J. Holder, R. C. Hiorns, N. Sommerdijk, S. J. Willims, R. G. Jones, and R. J. M. Nolte, *Chem. Commun.* 14, 1445 (**1998**).
46. M. Bodanszky and A. Bodanszky, The Practice of Peptide Synthesis, Springer: New York (**1984**), p. 1.
47. A. K. Das, A. Banerjee, M. G. B. Drew, S. Ray, D. Halder, and A. Banerjee, *Tetrahedron* 61, 5027 (**2005**).
48. CrysAlis, Oxford Diffraction Ltd., Abingdon, UK (**2006**).
49. G. M. Sheldrick, Shelxs97, and Shelxl97, *Acta Cryst. A* 64, 112 (**2008**).
50. P. Pandit, N. Chatterjee, S. Halder, S. K. Hota, A. Patra, and D. K. Maiti, *J. Org. Chem.* 74, 2581 (**2009**).
51. W. Yin and M. Z. Yates, *Langmuir* 24, 701 (**2008**).
52. L. M. Dell'Acqua-Bellavitis and R. W. Seigel, *Langmuir* 24, 957 (**2008**).
53. S. Ghosh and S. Verma, *Tetrahedron* 64, 6202 (**2008**).
54. R. H. Schmidt and K. Haupt, *Chem. Mater.* 17, 1007 (**2005**).
55. R. H. Schimdt, K. Mosbach, and K. Haupt, *Adv. Mater.* 16, 719 (**2004**).
56. I. Alfonso, M. Bru, M. I. Burguete, E. G. Verdugo, and S. V. Luis, *Chem. Eur. J.* 16, 1246 (**2010**).
57. J. Han, G. Song, and R. Guo, *Chem. Mater.* 19, 973 (**2007**).
58. E. Gazit, *FASEB J.* 16, 77 (**2002**).
59. J. K. Lee and B. R. Lentz, *Biochemistry* 36, 6251 (**1997**).
60. R. J. Mart, R. D. Osborne, M. M. Stevens, and R. V. Ulijn, *Soft Matter.* 2, 822 (**2006**).
61. R. A. Curtis, J. M. Prausnitz, and H. W. Blanch, *Biotechnol Bioeng.* 57, 11 (**1998**).
62. S. Ghosh, M. Reches, E. Gazit, and S. Verma, *Angew. Chem. Int. Ed.* 46, 2002 (**2007**).
63. P. Mukherjee, M. G. B. Drew, and A. Ghosh, *Inorg. Chem.* 48, 2364 (**2009**).
64. V. A. Klyachko and B. Jackson, *Nature* 418, 89 (**2002**).
65. W. A. Braell, *Proc. Natl. Acad. Sci. USA* 84, 1137 (**1987**).

Received: 2 December 2010. Accepted: 11 January 2011.

RESEARCH ARTICLE